Journal of The Electrochemical Society, **151** (5) G347-G352 (2004)
0013-4651/2004/151(5)/G347/6/$7.00 © The Electrochemical Society, Inc.

Etching AlAs with HF for Epitaxial Lift-Off Applications

M. M. A. J. Voncken,[a,z] J. J. Schermer,[a] A. T. J. van Niftrik,[a] G. J. Bauhuis,[a] P. Mulder,[a] P. K. Larsen,[a] T. P. J. Peters,[b] B. de Bruin,[b] A. Klaassen,[c] and J. J. Kelly[d,*]

[a]Department of Experimental Solid State Physics III, [b]Department of Inorganic Chemistry and [c]Department of Solid State Nuclear Magnetic Resonance, University of Nijmegen, 6525 ED Nijmegen, The Netherlands
[d]Debye Institute, Utrecht University, 3584 CC Utrecht, The Netherlands

The epitaxial lift-off process allows the separation of a thin layer of III/V material from the substrate by selective etching of an intermediate AlAs layer with HF. In a theory proposed for this process, it was assumed that for every mole of AlAs dissolved three moles of H_2 gas are formed. In order to verify this assumption the reaction mechanism and stoichiometry were investigated in the present work. The solid, solution and gaseous reaction products of the etch process have been examined by a number of techniques. It was found that aluminum fluoride is formed, both in the solid form as well as in solution. Furthermore, instead of H_2 arsine (AsH_3) is formed in the etch process. Some oxygen-related arsenic compounds like AsO, AsOH, and AsO_2 have also been detected with gas chromatography/mass spectroscopy. The presence of oxygen in the etching environment accelerates the etching process, while a total absence of oxygen resulted in the process coming to a premature halt. It is argued that, in the absence of oxygen, the etching surface is stabilized, possibly by the sparingly soluble AlF_3 or by solid arsenic.
 [DOI: 10.1149/1.1690293]

Manuscript received June 9, 2003. Available electronically March 26, 2004.

The epitaxial lift-off (ELO) process allows the production of single-crystalline thin films of III/V materials. The technique is interesting for the optoelectronics industry, because the use of thin film devices results in a more efficient transfer of generated heat from device to carrier or heat sink and significantly reduces the amount of material needed by reuse of the substrates. Furthermore, ELO allows the integration of III/V-based components with, *e.g.*, silicon-based devices.

In 1978, Konagai *et al.*[1] first reported on peeled-film technology (PFT); they separated a ± 5 μm thick GaAs epilayer from the GaAs substrate by etching a thin intermediate AlGaAs release layer with aqueous HF solution. It was found that this process stopped at certain depths, because etchant and reaction products could not be exchanged sufficiently fast through the narrow etch slit.[2] In 1987, Yablonovitch *et al.*[3] reported that for thinner epilayers with a thickness in the order of 1 μm this problem could be overcome by placing a droplet of black wax on top of the GaAs layer. The GaAs epilayers experience some stress due to the wax and curl up, thereby forcing open the small crevice between substrate and epilayer. As a result, the etch process, now referred to as ELO, no longer stopped at a certain depth. In a model to describe this process, Yablonovitch *et al.*[3] assumed that in etching AlAs release layers with HF solution in water each mole of AlAs forms three moles of H_2 gas and that the out-diffusion of this H_2 gas through the etch crevice is the limiting factor for the lateral etch rate. By assuming the rate of diffusion of H_2 out of the etch slit to be equal to the rate of production at the etch front, the maximum attainable etch rate was found to be

$$V_{e,max} = \frac{1}{\pi\sqrt{Rh/2}} \frac{Dn}{3N} \quad [1]$$

where N and n are the molar concentrations of AlAs and dissolved H_2, respectively, D the diffusion constant of H_2 in the solution, R the radius of curvature of the film, and h the thickness of the AlAs release layer, which generally varies between 3 and 50 nm. Maeda *et al.*[4] noted that, because of the diffusion coefficient in Eq. 1, $V_{e,max}$ is expected to increase exponentially with temperature. This diffusion coefficient is given by

$$D = D_0 e^{-E_a/kT} \quad [2]$$

with D_0 the diffusion coefficient at infinite temperature, E_a the activation energy, and k the Boltzmann constant. Using $E_a = 0.22$ eV[5] and $D(298\ K) = 4.8 \cdot 10^{-5}$ cm^2/s,[6] D_0 is found to be 0.25 cm^2/s. The combination of Eq. 1 and 2 and the substitution of constants, with $N = 0.037$ mol/cm^3[7] and $n = 0.63 \cdot 10^{-6}$ mol/cm^3[8] yield $V_{e,max}$ as a function of the process parameters R, h, and T

$$V_{e,max} = \frac{0.23}{\sqrt{Rh}} e^{-2551/T} \quad [3]$$

with $V_{e,max}$ in mm/h, R and h in mm, and T in K.[9] By application of a weight-induced epitaxial lift-off process (WI-ELO),[5,9] the relation between V_e and the relevant process parameters, according to Eq. 3, has been investigated. As far as the dependence of V_e on h and T is concerned, good qualitative agreement between theory and experiment was found, but a qualitative discrepancy was encountered for the relation between V_e and R. Furthermore, the lateral etch rate, as predicted by the model, showed a very large quantitative discrepancy with experiments. For a radius of curvature of 50 mm and a release layer thickness of 5 nm the model predicts a maximum attainable etch rate of approximately 3 μm/h at room temperature, while the experiments show values around 3 mm/h.[9] From this it was concluded[5,9] that the diffusion of hydrogen gas out of the etch crevice is not the limiting factor in the process, or that hydrogen may not even be a reaction product. This shows that for a correct description of the ELO process information about the actual etching reaction of AlAs with HF is essential.

The present study aims to clarify this reaction. For this purpose, layers of AlAs were etched with aqueous HF solution. The solid, aqueous, and gaseous reaction products were examined with a number of techniques. In previous WI-ELO experiments it was found that oxygen has an influence on the etch rate. For this reason the effect of ambient oxygen on the etch process has also been investigated.

Experimental

All samples used were grown on 2 in. undoped GaAs wafers with crystal orientation (100), 2 degrees off towards ⟨110⟩ using low-pressure metallorganic vapor-phase epitaxy (MOVPE) in an Aixtron 200 reactor. Source materials were trimethyl-gallium and trimethyl-aluminum for the group III and arsine for the group V elements. Disilane was used as the precursor of the *n*-type dopant silicon. The sample for the solid and aqueous reaction products

* Electrochemical Society Active Member.
z E-mail: maartenv@sci.kun.nl

analysis consisted of a layer of *n*-type AlAs of 50 μm thickness, capped with a 0.3 μm undoped GaAs layer. This cap layer was applied to prevent premature oxidation of the AlAs by oxygen in the air. The samples used for studying the gaseous reaction products and the influence of oxygen in the environment on the etch rate had a similar structure but an AlAs layer of only 5 μm thickness.

The sample for the solid and aqueous reaction products analysis was broken into smaller pieces, which were placed in an airtight stainless steel container, together with two stainless steel balls. This container was mounted in a shaker machine (Retsch MM200) and after 3 min of milling at a frequency of 30 Hz, the wafer was ground up finely enough for further processing. The AlAs/GaAs powder mixture was transferred to a glass vessel, and a stirring magnet was added. The vessel was closed with a rubber septum to prevent escape of any poisonous gas, which could be produced during the etch process. 2 mL of an aqueous 12% HF solution was added to the glass vessel with a syringe through the septum. This amount of HF ensures that four moles of HF are present for each mole of AlAs in the powder. Therefore, all the AlAs could react with the HF while leaving only a small amount of HF, so that the glass of the vessel would hardly be etched. Note that, compared to AlAs, the reaction rate of GaAs with HF is 10^6 times lower.[10] After the reaction was complete (1.5 h, as found in explorative experiments), the slurry, containing the fluid together with part of the fine solid remains of the wafer and some solid reaction products, was extracted and transferred to another glass vessel. This vessel was placed in a centrifuge for 5 min at 7000 rpm to separate the different fractions in the slurry. After the separation process, solid debris from the wafer, a white powder, a clear solution, and, floating on this solution, a thin film with a metal-like appearance were found form the bottom to the top of the vessel. The solution was examined using both aluminum nuclear magnetic resonance (NMR, Bruker Avance DRX500) and fluorine NMR (Bruker Avance DMX300) analyses. The NMR equipment was calibrated with an $[Al(H_2O)_6]^{3+}$ solution and with trifluoro-acetic acid, respectively. The white powder and the metal-like film were taken from the vessel to be examined with scanning electron microscopy (SEM), combined with energy dispersive spectroscopy (SEM-EDS). Additionally, an X-ray powder diffraction spectrum was obtained from the white powder, using a Philips PW1820 automatic powder diffractometer.

For the gas-chromatography measurements, half a wafer with a 5 μm thick AlAs layer was milled for 3 min at 30 Hz and etched with 2.5 mL of an aqueous 0.5% HF solution in a closed vessel. This ensures that a sufficient amount of HF is present to etch all the AlAs. After the reaction was complete, a 10 μL sample from the gas phase above the solution was extracted through the septum using a syringe and fed into both a gas chromatograph/mass spectrometer (GC/MS, Interscience Polaris Q with a 30 m Rtx-1 column) and a gas chromatograph with a flame ionization detector (GC/FID, Hewlett Packard HP6890 Plus with a 30 m HP-1 column). The latter gives flame conductivity as a function of the retention time. To test whether or not AsH_3 is formed in the reaction, a sample of arsine gas, taken directly from the gas system of the MOVPE reactor, was also fed into both the GCs for comparison of the signals. To test whether or not hydrogen is formed during the etch process, a sample from the reaction gas and a hydrogen calibration sample were fed into a gas chromatograph with a thermal conductivity detector (GC/TCD, Hewlett Packard HP 5890A with a Porapack Q (80-100 mesh, Supelco) column), which is particularly suited for the detection of hydrogen gas.

In a final series of experiments, the gas composition in the glass vessel was varied to find out whether or not the oxygen of the ambient atmosphere plays an active role in the etch process of AlAs with HF. For this purpose, three samples, each consisting of half a wafer with 5 μm of AlAs, were processed. The first and third samples were ground and etched under pure nitrogen to prevent oxidation of the AlAs, while the second sample was processed in air and etched in a pure oxygen atmosphere. A syringe was used to apply 2.5 mL aqueous 0.5% HF solution to samples 1 and 2 through the septum, thereby preserving the atmosphere in the vessel. The third sample was etched with an HF solution that was placed in a nitrogen environment and through which nitrogen gas was bubbled for an hour. In this procedure, almost all the oxygen was removed from the solution and hardly any residual oxygen was expected to be present during the etching process. A titration measurement afterwards confirmed that the nitrogen bubbling procedure had not changed the concentration of the HF solution. For an overview of the samples and the processing conditions, see Table I.

Table I. Conditions applied during preparation and etching of the samples used in the gas composition experiments.

	Processing conditions		
Sample	Grinding atmosphere	Etching atmosphere	HF solution
1	N_2	N_2	Kept under air
2	Air	O_2	Kept under air
3	N_2	N_2	N_2 bubbling

For each of the three samples, 10 μL gas samples were taken from the vessel in which the AlAs and HF were reacting, every 10 to 15 min during the first hour, and subsequently every 30 to 60 min, and fed into both the GC/MS and the GC/FID.

Results and Discussion

Solid reaction products; SEM-EDS and powder diffraction.—The SEM-EDS measurements revealed the presence of aluminum and fluorine in the white powder. Oxygen could not be detected with this particular SEM-EDS setup; it is therefore not possible to decide whether the powder consists of aluminum fluoride, aluminum oxide, or an oxyfluoride. The thin film contained gallium and arsenic. This is probably some very fine GaAs powder, which, due to surface tension, floated on the solution and thereby formed a film with a metal-like appearance.

X-ray powder diffraction analysis of the white powder revealed two different crystal forms of the compound $AlF_3 \cdot 3H_2O$ (rosenbergite and aluminum fluoride hydrate). It can therefore be concluded that aluminum fluoride is the only solid reaction product.

Aqueous reaction products; aluminum and fluorine NMR.—The result of the Al-NMR measurement is given in Fig. 1. A sharp peak around 0 ppm, identical to the reference signal from the reference measurement is attributed to $[Al(H_2O)_6]^{3+}$, the underlying wide band with a fwhm of ~650 Hz to either an $[AlF_n(H_2O)_{6-n}]^{(3-n)+}$ with $n = 0 \ldots 3$ or an $[Al_2(OH)_2(H_2O)_n]^{4+}$ with $n = 0 \ldots 4$ compound.[11] Comparing the tabulated data for the latter two com-

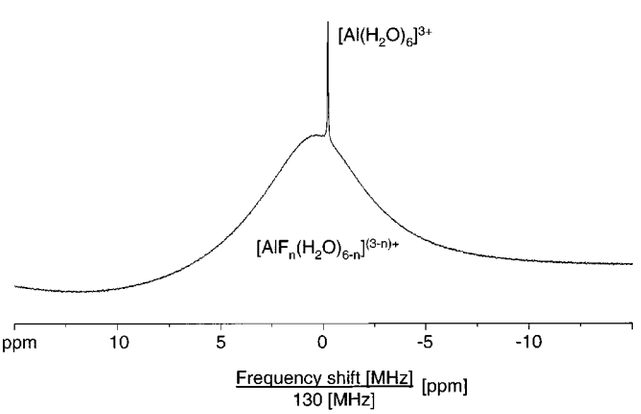

Figure 1. Aluminum NMR on the reaction products in solution. The measurement was performed at a frequency of 130 MHz. The sharp peak is attributed to $[Al(H_2O)_6]^{3+}$, the wide peak with a fwhm of ~650 Hz is attributed to an $[AlF_n(H_2O)_{6-n}]^{(3-n)+}$ with $n = 1 \ldots 3$ compound.

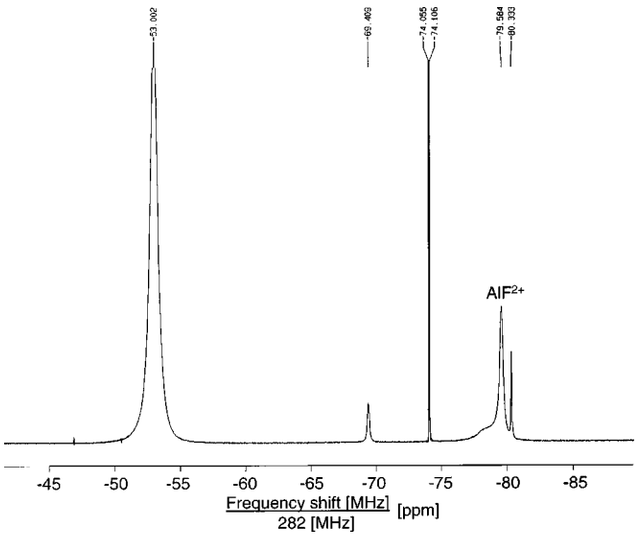

Figure 2. Fluorine NMR on the reaction products in solution. The measurement was performed at a frequency of 282 MHz. The peak at −79.6 ppm is attributed to an AlF^{2+} compound. Independent measurements on an aqueous HF solution and on NaF in water confirmed that the strong peak at −53.0 ppm stems from the F^- ion, while the peak at −80.3 ppm most likely originates from the undissociated HF. The origin of the other peaks is unknown.

pounds, we conclude that the chemical shift (+2 to +15 ppm for the fluoride and +3 ppm for the hydroxide) cannot be used to distinguish between the two. The tabulated line widths (550 Hz for the fluoride and 450 Hz for the hydroxide) indicate a better match of the fluoride with the measurements. Additionally, since the formation of a hydroxide compound in a strongly acidic environment ($pH < 2$) is rather unlikely,[12] it can be deduced that the fluoride compound is the reaction product measured. Further evidence for this was found in the fluorine-NMR measurement (see Fig. 2). Several peaks are detected, and the peak at −79.6 ppm is attributed to an AlF^{2+} compound.[13] From these results it is concluded that during HF etching of AlAs, solid aluminum fluoride hydrate ($AlF_3 \cdot 3H_2O$) and dissolved aluminum fluoride compounds ($[AlF_n(H_2O)_{6-n}]^{(3-n)+}$ with $n = 0 \ldots 3$) are produced.

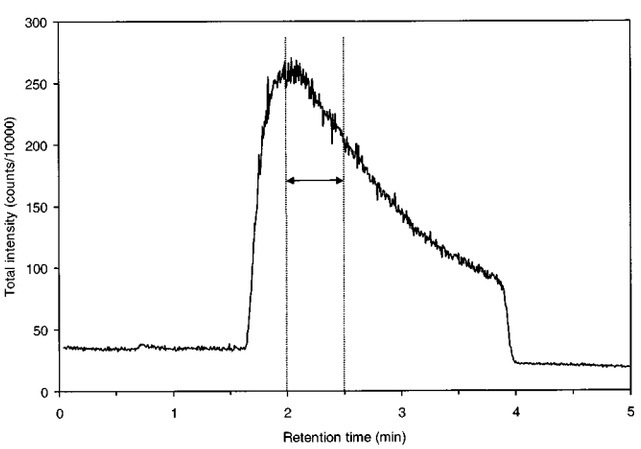

Figure 3. Retention time *vs.* total intensity for a GC/MS measurement. It is shown that the typical retention time for the gaseous reaction products is between 1 min, 38 s and 4 min. Signals from 2 to 2.5 min were considered for further analysis.

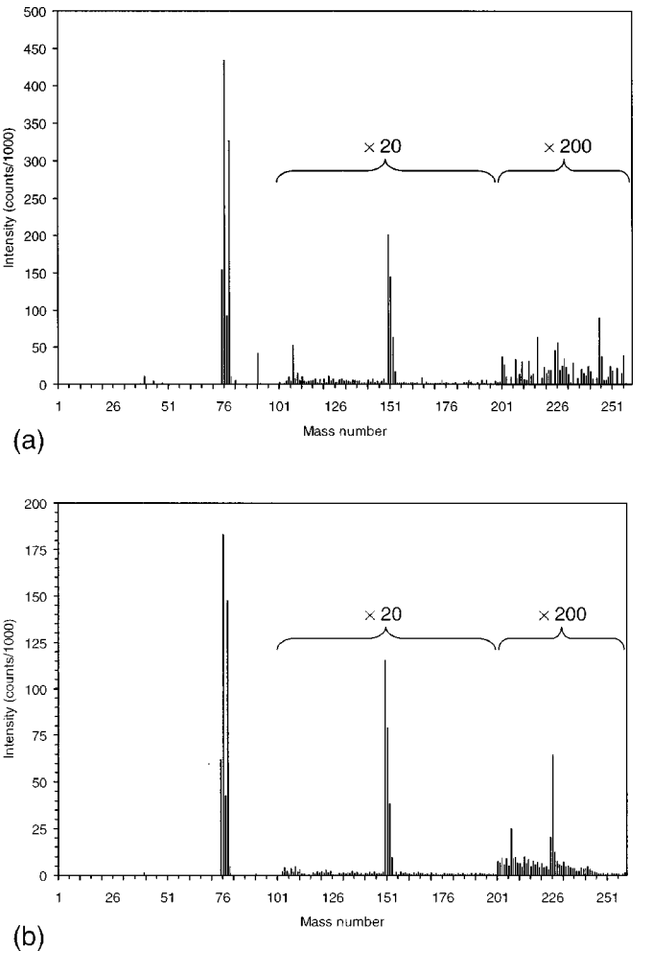

Figure 4. Mass spectrum for the gaseous reaction products (a) and for arsine (b). Values below mass 35 have been omitted. For mass values of 101 to 200, the intensity has been multiplied by 20, for mass values of 201 and higher, the intensity has been multiplied by 200.

Gaseous reaction products; gas chromatography.—The GC/MS measurements yield a three-dimensional diagram showing retention time *vs.* mass number *vs.* intensity (counts). In a two-dimensional projection, as given in Fig. 3, the intensities for all mass numbers are added. The reaction gas signal appears to lie between 1 min, 38 s and 4 min. For further analysis, the average signal before injection of the reaction gas and after the reaction gas has passed the chromatography column is subtracted from the reaction gas signal in order to eliminate all possible background signals. Furthermore, only the signal collected between 2 and 2.5 min retention time is used, in order to obtain measurements that are as reproducible as possible. The mass spectrum for this time frame is given in Fig. 4a. Mass numbers below 35 are omitted, because some of the main peaks in this region (nitrogen, oxygen, and water) are so strong that they render the peaks of several of the reaction products virtually indistinguishable on the same scale. Figure 4b shows a spectrum for arsine gas, diluted in nitrogen, taken from the gas system of the MOVPE reactor. Arsine has a mass number of 78; the peaks at 79, 77, 76, and 75 are attributed to several ionized forms of AsH_3 (AsH_4^+, AsH_2^+, AsH^+, and As^+, respectively), which are easily formed in the mass spectrometer. The peaks around 150 and around 225 are attributed to arsenic dimers and trimers. A comparison of Fig. 4a and b shows that the arsine signature from Fig. 4b is predominantly present in Fig. 4a, indicating that arsine gas is a major reaction product in the reaction of AlAs with an aqueous HF solu-

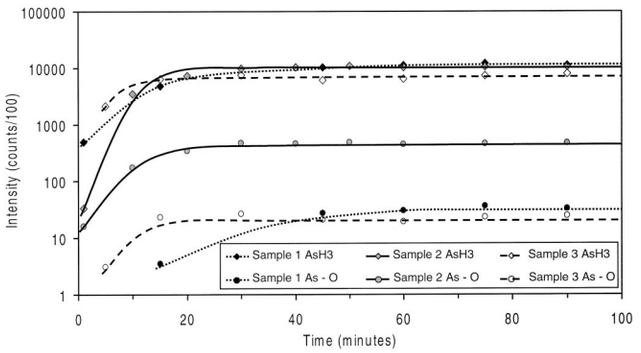

Figure 5. Time dependence of the GC/MS sum intensity for arsine (mass numbers 75 to 79, 150 to 153, and 225 to 229) and the oxygen-related arsenic compounds (mass numbers 91, 92, and 107). Samples 1 and 3 were milled and etched in a nitrogen environment (the etchant for sample 3 was deaerated), sample 2 was milled in air and etched in an oxygen environment, respectively. Sample 3 was etched in deaerated HF solution.

tion. Other reaction products with mass numbers of 91, 92, and 107 can be coupled to the oxygen-related arsenic species AsO^+, $AsOH^+$, and AsO_2^+, respectively. These species are most likely formed by ionization in the GC/MS of a single compound, like As_2O_3. This assumption is supported by the fact that the GC/FID only shows one peak for the whole range of oxygen-related arsenic compounds. For arsine, this is also the case, since the GC/MS shows peaks at 75 to 79, 150 to 153, and at 225 to 229, whereas the GC/FID only shows one peak.

Injection of the reaction gas and a calibration sample into the GC/TCD, suited for hydrogen detection, showed an H_2 concentration of 0.053% in a 55 mL vessel, resulting in a total amount of 1.19 μmol. Because 170 μmol AlAs was dissolved in the vessel, this would mean that each mole of AlAs yielded only 0.007 mole of hydrogen gas. From this it can be concluded that, contrary to previous assumptions,[3] H_2 is not a major reaction product in the etch process of AlAs with HF. Diffusion of hydrogen out of the etch crevice therefore cannot be the limiting factor for lateral etching in the ELO process. The hydrogen detected is either the background concentration or it is formed as a secondary reaction product by partial decomposition of AsH_3 to solid arsenic and hydrogen gas.

Influence of oxygen on the etch process.—The influence of oxygen on the reaction was found by examining the total intensity of arsine (75 to 79, 150 to 153, and 225 to 229 added) and of the oxygen-related arsenic compounds (91, 92, and 107 added) over time. In Fig. 5, the summation of these mass-spectrometer intensities *vs.* time are given for samples 1 to 3. Note that the vertical axis in Fig. 5 has a logarithmic scale. Comparison of the increase in AsH_3 intensity over time for the three samples shows that sample 1 and sample 2 reach the same final intensity. In the etching of sample 1, however, more time is needed to reach this final intensity, indicating that the presence of oxygen enhances the reaction rate. From the fact that the arsine intensity of sample 1 reaches the same final level as that of sample 2, it can be concluded that oxygen in the HF solution (about 1 mole of oxygen for every 50 moles of AlAs) acts catalytically, or that it reacts in very small quantities. Sample 3, which was etched with HF solution purged of dissolved oxygen, shows a very fast increase up to its maximum arsine intensity, but this maximum intensity is significantly lower than that of the other two samples. This indicates that the etching process was blocked before all the AlAs was etched.

Comparison of the intensity increase with time for the oxygen-related arsenic compounds shows a clear difference between sample 2 and the other two samples. If oxygen is present in excess, these compounds are formed in much larger quantities than when very little or no oxygen is present. The formation of the oxygen-related arsenic compounds reaches the lowest level if the sample is etched with an oxygen-free HF solution (sample 3). The fact that an oxygen-containing species is still formed, although no oxygen whatsoever should be present, can be explained by possible small leaks in the rubber septum, resulting in very small amounts of oxygen diffusing into the vessel, and by the fact that it is not possible to remove all oxygen from the HF solution, simply by bubbling nitrogen gas through it. The lower intensity of the oxygen-related arsenic compounds in the case of sample 3 compared to sample 1 may partly be due to the fact that less oxygen is present, and therefore less of these compounds can be formed. Another effect is that, in case of sample 3, probably not all AlAs was etched in the reaction, as was observed in the intensity plots for arsine. As a result, less arsenic is freed and less of the compounds can be formed.

For all experiments, except that of sample 3, GC/FID measurements show two peaks at retention times of 2 min, 6 s and at 2 min, 9.6 s, respectively. For the gas retrieved from the etching of sample 3, only one peak at a retention time of 2 min, 6 s is observed. Injection of pure arsine from the gas system of the MOVPE reactor also resulted in one peak at 2 min, 6 s. From these results it can be concluded that arsine is formed in all cases. For samples 1 and 2, processed with a significant amount of oxygen, the formation of one other component is detected. This is most likely the set of oxygen-related arsenic components with mass numbers 91, 92, and 107. For sample 3 the concentration of oxygen-related arsenic species, which according to GC/MS measurements is half of that obtained by sample 1, is obviously below the detection limit of the GC/FID equipment.

Reaction mechanism and stoichiometry.—From the investigation of solid reaction products and the reaction products in solution it can be concluded that $[Al(H_2O)_6]^{3+}$, and aluminum fluoride compounds $[AlF_n(H_2O)_{6-n}]^{(3-n)+}$ with $n = 1 \ldots 3$ are formed. Judging from the formation of $AlF_3 \cdot 3H_2O$ powder, present in the vessel, we must conclude that the fluorine compound does not have a high solubility in water or in an HF solution.

The analysis of the gaseous reaction products clearly shows the formation of arsine (AsH_3) gas. A number of oxygen-related arsenic compounds, such as AsO, AsOH, and AsO_2, are also detected at low concentrations with the GC/MS, if oxygen is not excluded during the preparation of the samples. From the analysis of gaseous reaction products, formed in the etching process under different atmospheres, it can be concluded that (*i*) no hydrogen is formed in etching AlAs with HF and (*ii*) the presence of oxygen is necessary for completing and maintaining the reaction.

Etching of AlAs in HF solution with the formation of AsH_3 seems similar to the etching of InP in concentrated HCl solution.[14] In the latter case chemical attack by undissociated HCl on InP surface bonds gives rise to the formation of PH_3 and $InCl_3$

$$InP + 3HCl \rightarrow InCl_3 + PH_3 \qquad [4]$$

The InP is subsequently hydrated. In principle, etching of AlAs in the present work could be due to either the undissociated acid (HF or HF_2^-) or the dissociated species (H^+ and F^- ions). In order to check these possibilities, AlAs etch experiments were performed in both concentrated HCl solution (with a high content of undissociated acid)[14] and in 10% HCl solution (which only contains H^+ and Cl^- ions). In both cases fast etching of AlAs was observed with the formation of considerable amounts of arsine. This result suggests that dissociated HF should be capable of dissolving AlAs.

Because of the difference in electronegativity of Al and As, the Al-As surface bond is expected to be polarized. Proton attack on the negatively charged As leads to the rupture of the Al-As bond and the formation of a new As-H bond (step 1 of Fig. 6a). At the same time, the positively charged Al can be complexed by either F^- (step 2) or

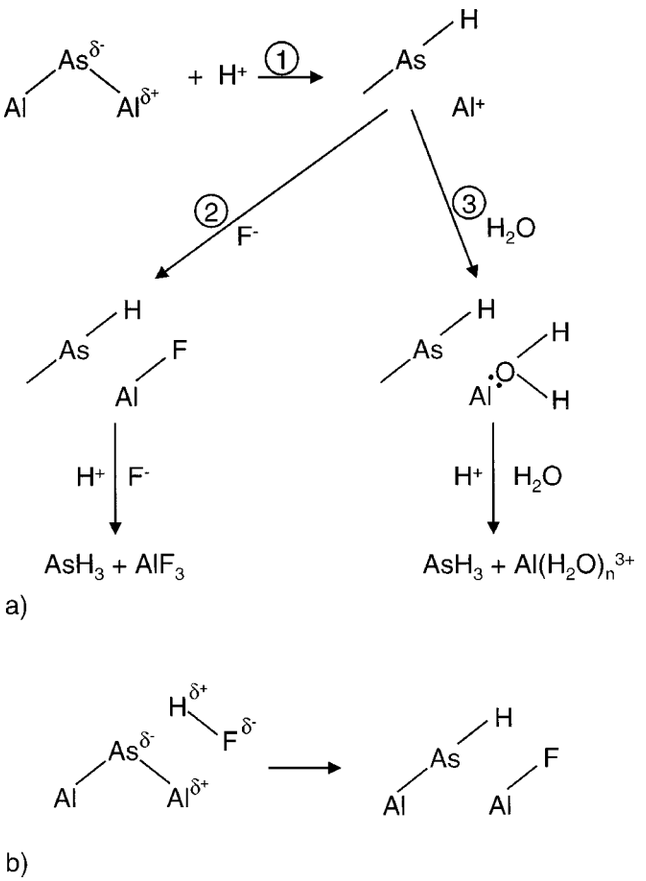

Figure 6. Reaction mechanism for the etching of (a) AlAs with dissociated HF and (b) for undissociated HF.

H_2O (step 3). If the remaining back bonds to As and Al react in the same way as in steps 1 to 3, then AsH_3 and either AlF_3 or $Al(H_2O)_n^{3+}$ will be formed. Alternating attack on a surface Al atom by F^- and H_2O will give rise to a mixed fluoro-aqua complex $[AlF_n(H_2O)_{(6-n)}]^{(3-n)+}$, with $n = 1 \ldots 3$.

In principle, attack on a surface Al-As bond by the undissociated acid, as occurs for InP in HCl, is also possible (see Fig. 6b). The result will be the same as for step 2 of Fig. 6a. Subsequent reactions with F^- or HF and/or H_2O will lead to the same products.

The results of the present work clearly show that the AlF_3 product is only sparingly soluble. The formation of an insoluble trifluoride (which may be in the hydrated form, see the NMR results) can explain the passivation, which is observed in this system. The fact that passivation does not occur if AlAs is etched with HCl resulting in AsH_3 and $AlCl_3$ shows that arsenic hydride is unlikely to be responsible for the termination of etching. Also the $AlCl_3$ formed in this case will rapidly hydrolyze and dissolve (similar to HCl etching of InP). From the results obtained in aerated and deaerated solutions it is clear that oxygen plays a role in the surface chemistry. Direct oxidation of A1As by oxygen can occur to a limited extent (this would explain the As_2O_3 detected in the GC/MS experiments). The presence of adsorbed oxygen is expected to influence the etching steps, as shown in Fig. 6. The results suggest that passive film ($A1F_3$) formation is hindered; why this is so is not clear at present.

Another possible explanation for the observed passivation is the formation of solid arsenic at the surface. The oxygen, which is present in the solution, might oxidize the arsenic to form As_2O_3 as detected in the GC/MS and thus prevent passivation and maintain the etch process.

Conclusions

In previous reports on the epitaxial lift-off process it was assumed that in etching AlAs with HF solution three moles of hydrogen are formed for each mole of AlAs. In the present study, this has been investigated by a structural analysis of all reaction products, solid, in solution, and gaseous. SEM-EDS and X-ray diffraction measurements show that a white powder, formed during the etching, is an aluminum fluoride compound. Aluminum and fluorine NMR experiments on the solution showed the presence of the aluminum species $[AlF_n(H_2O)_{6-n}]^{(3-n)+}$, with $n = 1 \ldots 3$ and $[Al(H_2O)_6]^{3+}$. Gas chromatography measurements with GC/MS and with GC/FID show the formation of arsine and oxygen-related arsenic compounds like AsO, AsOH, and AsO_2. The latter compounds are probably formed when As_2O_3 decomposes in the GC/MS, an assumption that is supported by the fact that the GC/FID shows only one peak for these compounds. The GC/TCD experiments refute the assumption that hydrogen gas is formed in the etch process. Consequently, the out-diffusion of hydrogen through the narrow etch slit cannot be the limiting step in the lateral etch rate of the epitaxial lift-off process.

Oxygen is shown to play a significant role in the ELO etch process. During an *in situ* measurement in an aerated solution it is found that the amount of arsine gas increases faster to its maximum, if a sample is etched in an oxygen atmosphere. If the process is performed in a nitrogen atmosphere, the same maximum value is reached, but the time needed to reach this value is considerably longer. If, in addition, the oxygen dissolved in the HF solution is first removed, the arsine concentration reaches its maximum considerably faster, but this maximum value is much lower than that found in the presence of oxygen.

From experiments in which AlAs was etched with both concentrated and diluted (10%) HCl, it was found that the dissociated acid is capable of dissolving AlAs. The mechanism describing the etching of AlAs with aqueous HF solution is therefore similar. In a first step, the proton attack on the As leads to a rupture of the As-Al bond and an As-H bond is formed. The positively charged Al is at the same time complexed by either F^- or H_2O. The remaining Al and As back bonds may react in a similar way to form AlF_3 or $Al(H_2O)_n^{3+}$ compounds. Alternating attacks on a surface Al atom by F^- and H_2O will give rise to a mixed fluoro aqua complex $[AlF_n(H_2O)_{(6-n)}]^{(3-n)+}$, with $n = 1 \ldots 3$. Etching of AlAs by undissociated HF is in principle also possible. The reaction mechanism is then similar to the etching of InP in concentrated HCl and the process yields the same reaction products as for the etching of AlAs in a dissociated HF solution.

The AlF_3 compound that is formed in the reaction is shown to be sparingly soluble in water. The formation of this compound at the surface can therefore explain the passivation, as observed in this process. Another possible passivating agent is solid arsenic at the surface. The oxygen in the solution might oxidize the arsenic to form As_2O_3 as is detected in the GC/MS and thus prevent passivation.

The model, as described above, is confirmed by examination of the ELO process in its normal implementation. In that case, the release layer is extremely thin (~5 nm), so that blocking of the AlAs surface plays an extremely important role. In experiments, it was found that this process comes to a premature halt, when absolutely no oxygen is present during etching. With oxygen present, the process continues and the III/V films are freed from their substrate.

It should be clear that an understanding of the epitaxial lift-off process requires more than knowledge of the reaction mechanism and stoichiometry. Interesting points for further investigation in-

clude the influence of stress and strain on the lateral etch rate and the escape of the gaseous reaction products.

Acknowledgments

The authors thank Dr. H. op den Camp (Department of Microbiology, University of Nijmegen) for the GC/TCD measurement on hydrogen and J. Joordens and A. Swolfs (Department of Biophysical Chemistry, University of Nijmegen) for their help on the aluminum and fluorine NMR measurements, respectively. Dr. J. Fransen (Nijmegen Center for Molecular Life Sciences, University of Nijmegen) is acknowledged for the SEM-EDS measurements. J. M. M. Smits and Dr. R. de Gelder (Crystallography Group, Department of Inorganic Chemistry, University of Nijmegen) are acknowledged for the powder diffraction measurement. The authors thank Dr. P. H. M. Budzelaar (Department of Inorganic Chemistry, University of Nijmegen) for helpful discussions on the reaction mechanism and the critical reading of the manuscript.

University of Nijmegen assisted in meeting the publication costs of this article.

References

1. M. Konagai, M. Sugimoto, and K. Takahashi, *J. Cryst. Growth*, **45**, 277 (1978).
2. J. C. C. Fan, *J. de Physique*, **43**, C1-327 (1982).
3. E. Yablonovitch, T. Gmitter, J. P. Harbison, and R. Bhat, *Appl. Phys. Lett.*, **51**, 2222 (1987).
4. J. Maeda, Y. Sasaki, N. Dietz, K. Shibahara, S. Yokoyama, S. Miyazaki, and M. Hirose, *Jpn. J. Appl. Phys., Part 1*, **36**, 1554 (1997).
5. J. J. Schermer, G. J. Bauhuis, P. Mulder, W. J. Meulemeesters, E. Haverkamp, M. M. A. J. Voncken, and P. K. Larsen, *Appl. Phys. Lett.*, **76**, 2131 (2000).
6. *Kirk-Othmer Encyclopedia of Chemical Technology*, Vol. 13, 4th ed., Wiley, New York (1995).
7. *Properties of Aluminium Gallium Arsenide*, S. Adachi, Editor, EMIS Datareviews Series No. 7, INSPEC, London, (1993).
8. *Treatise on Analytical Chemistry*, I. M. Kolthoff, P. J. Elving, and E. B. Sandell, Editors, Part II, Vol. 1, Interscience, New York (1961).
9. M. M. A. J. Voncken, J. J. Schermer, G. Maduro, G. J. Bauhuis, P. Mulder, and P. K. Larsen, *Mater. Sci. Eng., B*, **95**, 242 (2002).
10. M. M. A. J. Voncken, J. J. Schermer, G. J. Bauhuis, P. Mulder, and P. K. Larsen, *Appl. Phys. A: Mater. Sci. Process*, In press.
11. *NMR and the Periodic Table*, R. K. Harris and B. E. Mann, Editors, Academic Press, London (1978).
12. *Advanced Inorganic Chemistry*, 6th ed., F. A. Cotton, G. Wilkinson, C. A. Marillo, and M. Bochmann, Editors, p. 183, John Wiley & Sons, New York (1999).
13. N. A. Matwiyoff and W. E. Wageman, *Inorg. Chem.*, **9**, 1031 (1970).
14. P. H. L. Notten, *J. Electrochem. Soc.*, **131**, 2641 (1984).